Optimized Local Control for Active Distribution Grids using Machine Learning Techniques

Federica Bellizio[*], Stavros Karagiannopoulos[*], Petros Aristidou[§], Gabriela Hug[*]
[*]EEH - Power Systems Laboratory, ETH Zurich, Physikstrasse 3, 8092 Zurich, Switzerland
[§]School of Electronic and Electrical Engineering, University of Leeds, Leeds LS2 9JT, UK
Emails: bellizif@student.ethz.ch, {karagiannopoulos, hug}@eeh.ee.ethz.ch, p.aristidou@leeds.ac.uk

Abstract—**Modern distribution system operators are facing a changing scenery due to the increasing penetration of distributed energy resources, introducing new challenges to system operation. In order to ensure secure system operation at a low cost, centralized and decentralized operational schemes are used to optimally dispatch these units. This paper proposes a decentralized, real-time, operation scheme for the optimal dispatch of distributed energy resources in the absence of extensive monitoring and communication infrastructure. This scheme uses an offline, centralized, optimal operation algorithm, with historical information, to generate a training dataset consisting of various operating conditions and corresponding distributed energy resources optimal decisions. Then, this dataset is used to design the individual local controllers for each unit with the use of machine learning techniques. The performance of the proposed method is tested on a low-voltage distribution network and is compared against centralized and existing decentralized methods.**

I. INTRODUCTION

Distribution Network Operators (DNOs) are facing new challenges caused by the increasing penetration of Distributed Energy Resources (DERs) in medium and Low Voltage (LV) networks. On the one hand, new DERs connected at the distribution level, such as PhotoVoltaic generators (PVs), can increase the variability of power injections leading to voltage and thermal overload issues. On the other hand, controllable DERs can provide operational flexibility assisting the DNOs in satisfying their grid constraints and deferring network investments. In addition, they can enable the DNO to provide ancillary services to the transmission network, thus upgrading the passive role of traditional Distribution Networks (DNs).

Several DER active control measures have been considered in the literature, including Reactive Power Control (RPC) [1], Active Power Curtailment (APC) [2], Battery Energy Storage Systems (BESS) and Controllable Loads (CLs) [3], or combinations of these [4]. The operation schemes proposed to control the DERs can be classified into centralized or decentralized based on the available monitoring and communication infrastructure and the location of the decision making process.

In centralized DN operation schemes, a fully controllable and observable grid is assumed allowing for the use of network-level optimization strategies. In these schemes, a central controller relies on communication infrastructure to employ network-level optimization and provide system-wide optimal setpoints for all controlled DERs. These strategies usually rely on the solution of Optimal Power Flow (OPF) formulations for DNs. Some of the most important challenges of these problems are the consideration of the non-convex non-linear AC power flows in the OPF framework, the inclusion of discrete (integer) decision variables, and the operation of DNs under uncertainty, all of which can easily make the problem computationally complex.

Nevertheless, DN OPF formulations have gained a lot of attention in recent years due to advances in computational power and theoretical developments in approximating the non-linear AC power flow equations. Different techniques have been used to tackle this problem, such as semi-definite relaxations [5], heuristics, or linear approximations [6]. In this work, we will use an iterative method, based on the Backward/Forward Sweep (BFS) power flow [7]–[9].

In decentralized DN operation schemes, only local information is used to dictate the DER response without the need for a central controller or communication. These local control schemes yield suboptimal results compared to centralized methods due to the reduced observability, but they are simpler to implement, more cost effective, and resilient. In these schemes, the DERs react to local measurements according to some predefined rules. They have been widely explored in the literature [1], [2], [10] and have already been incorporated into some grid-codes and standards [11]; mainly with the objective to mitigate voltage problems. Most often, DERs are used to provide reactive power support based on local terminal voltage measurements, i.e. $Q = f(V)$ [10], or combined voltage and active power injection measurements, i.e. $Q = f(V, P)$ [12]. Other techniques involve adjusting the power factor according to their active power injection, i.e $cos(\phi) = f(P)$ [11]. When reactive power compensation is not sufficient to mitigate the voltage issues, APC can also be employed based on voltage measurements, i.e. $P_{curt} = f(V)$ [2], [12]. Other more simplified approaches include a fixed power factor mode, or fixed reactive power consumption. Figure 1 shows some typical DER APC and RPC characteristic curves to control the voltage in DNs.

However, these decentralized control schemes are identical for all DERs and do not consider their location or network-wide challenges. For this reason, a hybrid approach was introduced in [3], [13], where an off-line centralized optimization is used to drive the development of local control schemes. In this approach, each DER behaves according to local measurements and informed from historical data available from off-line analysis, thus trying to mimic the behaviour of optimal centralized solutions without the need for extensive communication. A similar approach is presented in [14], where regression is used to calculate a function for each inverter that maps its local historical data to pre-calculated optimal reactive power injections.

In this paper, a decentralized control scheme is proposed for the real-time control of DERs in DNs to achieve network-wide optimal and secure operation without the use of communication infrastructure. The design of the control scheme is performed in two stages. First, a centralized, OPF-based, operation scheme is used with historical data to generate a sequence of optimal DER setpoints at different operating conditions. The OPF formulation takes into consideration various active control measures as well as uncertainty coming from renewable generation and loads. Second, the generated dataset is used with supervised Machine Learning (ML) techniques
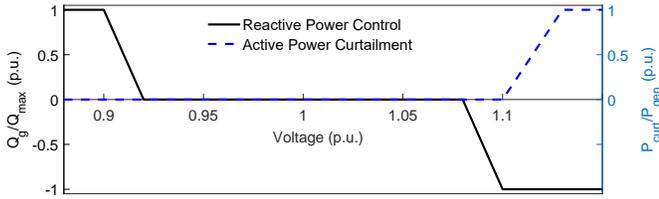
Fig. 1. Typical DER characteristic curves for active power curtailment and reactive power control.

for the development of DER controllers that use only local information to achieve near-optimal DN control in real-time operation.

The main contributions of the paper are as follows. First, we extend the centralized methodology of [4] to account for load uncertainties. Second, we propose a ML-based approach to derive the characteristic curves of each DER controller to be used in real-time operation. Finally, we propose a rule-based, local control scheme for the BESS operation. We demonstrate the performance of the proposed decentralized operation scheme on a typical European LV grid.

The remainder of the paper is organized as follows. Section II provides an overview of the chance constrained multi-period centralized OPF and the consideration of load uncertainty. Section III describes the derivation of the characteristic curves based on ML techniques, and Section IV introduces the considered case study and the simulation results. Finally, conclusions are drawn in Section V.

II. CHANCE CONSTRAINED MULTI-PERIOD OPF

In this section, we describe the first stage of the decentralized controller design. The chance constrained, multi-period, centralized OPF algorithm presented in [4] is used on forecasted and historical data to generate a dataset of optimal DER outputs at different operating conditions. This dataset is used in the second stage of the design to extract the local DER controller characteristic curves.

The centralized method, called BFS-OPF, is sketched in the upper part of Fig. 2 and consists of two parts: the multi-period OPF solution and the tightening of the constraints to treat uncertainty. First, a single iteration of the BFS power flow is incorporated within the multi-period OPF to replace the non-linear and non-convex AC power flow equations. After the optimal setpoints of the OPF problem are obtained, a full power flow solution is performed to update the new operating point. This procedure is repeated until convergence in terms of the maximum voltage magnitude mismatch is reached.

To capture the uncertainty coming from the stochastic nature of PV power injections, the optimization framework in [4] employs chance constraints for the voltage and current violations. Then, the voltage magnitude and current loading constraints are reformulated using the notion of tightenings, which represent security margins against uncertainty [15]. The tightenings are evaluated in the second iterative loop outside the OPF, using Monte Carlo (MC) simulations. The iterative procedure continues until all parts have reached convergence. The full BFS-OPF formulation and solution are described in [4].

In this work, we extend the formulation of [4] to also consider load uncertainty. That is, to evaluate the uncertainty margins in the BFS-OPF, both the DER and the load power injections are used, assuming that the corresponding uncertainty distributions are independent. The PV forecast error distribution is based on historical data of a specific location [16]. To compute the load uncertainty, we first implement a Feed-Forward Artificial Neural Network (ANN) [17], [18] to forecast the load consumption. As input to the ANN, we use historical daily load data in hourly steps from the same season and information about weekdays/weekends. In this way, we account for different patterns in demand due to different weather conditions and other seasonal effects. As output, we derive daily hourly load predictions. The Levenberg-Marquardt algorithm [19] is chosen as the implementation method, and the training automatically stops when the Mean Squared Error (MSE) of the validation samples stops improving. For each hour of the forecasted day, the forecast error can then be calculated by the difference between the actual and the predicted values.

Finally, the load uncertainty is included in the chance constrained BFS-OPF problem similarly to the PV generation uncertainty in [4] using a MC procedure.

III. DESIGN OF DER CHARACTERISTIC CURVES

In this section, we detail the derivation of the optimized local characteristic curves with the use of ML-techniques, obtained by post-processing the dataset generated with the centralized BFS-OPF algorithm of Section II. In order to find the best fitting in terms of out-of-sample performance, different analytical and statistical procedures are explored.

A. Support Vector Regression method

Several ML algorithms can be used for fitting purposes, such as Kernel ridge regression, random forest or K-nearest
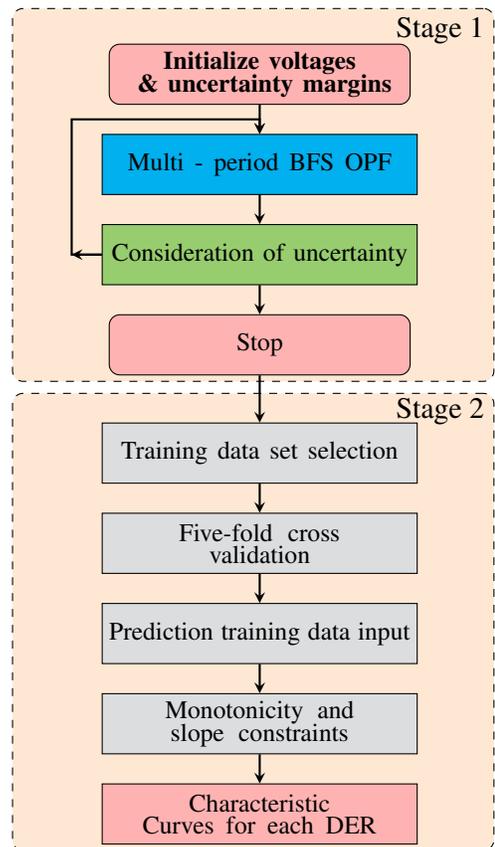
Fig. 2. Decentralized control design algorithm.

neighbors. The choice of the most suitable algorithm depends on the trade-off between specific characteristic requirements and the objectives. The supervised ML technique Support Vector Regression (SVR) was selected in this work. It is able to construct a model that deviates from the measured data by a value no greater than a predetermined amount ϵ. Furthermore, we focus on characteristic curves of the type $Q = f(V, P)$ and $P_{\text{curt}} = f(V, P)$ (see Fig. 1) and evaluate the fitting performance based on the distance to the OPF solution, with emphasis on critical noon hours with high PV injections. That is, the characteristic curves rely only on the measured local voltages to obtain the inverter q^g setpoints, which are given by

$$q^g = f(v). \tag{1}$$

The dataset with the optimal setpoints for different operating conditions that was generated by the offline BFS-OPF algorithm, can be reduced to a sequence $(v_1, q_1^g), ..., (v_n, q_n^g)$. A training set T is then selected to include only the setpoints corresponding to active power injections above a specific threshold (P_{thr}). This is given by

$$T = \{(v_t, q_t^g) \in \mathbb{R} \times \mathbb{R} : p_t^g \geq P_{thr}\}, \quad \text{with} \quad t \in [1, ..., n]. \tag{2}$$

The SVR can be used to calculate a function that is "as flat as possible", but deviates at most a distance of ϵ from all the training outputs $q_i^g \in T$. For the linear function

$$f(v) = \langle w, v \rangle + b \tag{3}$$

the convex optimization problem below is formulated to minimize the Euclidean norm of w:

$$\begin{aligned}
\min \quad & \frac{1}{2} w^T w + C \sum_{i=1}^{n} (\zeta + \zeta^*) \\
\text{s.t.} \quad & q_i^g - \langle w, v_i \rangle - b \leq \epsilon + \zeta, \quad \forall (v_i, q_i^g) \in T \\
& \langle w, v_i \rangle + b - q_i^g \leq \epsilon + \zeta^*, \quad \forall (v_i, q_i^g) \in T. \\
& \zeta, \zeta^* \geq 0
\end{aligned} \tag{4}$$

where the constant C penalizes the predictions outside the region defined by ϵ, and the slack variables (ζ, ζ^*) are used to allow some prediction errors.

In this work, the generalized, non-linear, version of the SVR is used [20]. The generalization is done with the introduction of functions, called Kernels, which map the training set into a new higher dimensional space, $\phi : T \rightarrow \mathcal{X}$, before applying the normal SVR described above. Different kernel functions [20] are used to model the training set:

- Linear: $\langle v, v' \rangle$ with C as free parameter;
- Polynomial: $(\gamma \langle v, v' \rangle + r)^d$ with C and the polynomial order d as free parameters;
- Radial-Basis Function (RBF): $exp(-\gamma |v - v'|)^2$ with C and the kernel scale γ as free parameters.

Then, for each individual DER controller, the kernel with the lowest overall out-of-sample MSE is identified through a five-fold cross validation process by optimizing the corresponding free parameters according to the Bayesian optimization [21]. Finally, for each measured local voltage of the input dataset, the corresponding reactive power injection is predicted according to the trained model $\mathcal{F}$, obtaining the $Q = f(V, P)$ characteristic curve:

$$\mathcal{F} : v_i \rightarrow \mathcal{F}(v_i) \qquad \forall i \in [1, ..., n] \tag{5}$$

The procedure determining the $P_{\text{curt}} = f(V, P)$ characteristic curves for each inverter-based DER is identical.

B. Characteristic curve post-processing

Both the resulting local characteristics should satisfy additional constraints to ensure a stable real-time operation. These are:

1) The local curves should respect under- and over- voltage protection limits that are the same for all inverters and define the curves in the areas with very low and high voltages, similar to Fig. 1.
2) The rate of change of the curves should be limited to avoid oscillatory behaviour and instability. That is,

$$\left| \frac{(f(v_j) - f(v_i))}{(v_j - v_i)} \right| \leq \phi_{crit}, \quad \forall v_i \leq v_j, \text{with} \quad i, j \in [1, ..., n] \tag{6}$$

3) The curves should be monotonic, following the description reported in Section I. More specifically, the $Q = f(V, P)$ characteristic curves should obey

$$f(v_i) \geq f(v_j), \quad \forall v_i \leq v_j, \text{with} \quad i, j \in [1, ..., n]. \tag{7}$$

A similar condition holds for the corresponding non-decreasing constraints of the $P_{\text{curt}} = f(V, P)$ curves.

C. Real-time operation of BESS

The real-time operation of the inverter-based DERs is dictated by the $Q = f(V, P)$ and $P_{\text{curt}} = f(V, P)$ characteristic curves extracted as described in the previous section. In addition, the behaviour of the BESS is dictated by a rule-based control scheme proposed in Algorithm 1.

More specifically, BESS charging is prioritized against APC, in order to avoid curtailing excess active power. This offers an alternative effective solution for peak demand shaving and voltage regulation to the rule-based control presented in [22]. According to Algorithm 1, once the local PV generation $P_{\text{PV,t}}$ exceeds the initial local load $P_{\text{l,t}}$, the BESS is charging and the final active power demand $P_{\text{net,t}}$ increases by the charging power $P_{\text{B,t}}^{\text{ch}}$. On the other side, when the local load exceeds generation, the BESS is discharged and $P_{\text{net,t}}$ decreases by the discharging power $P_{\text{B,t}}^{\text{dis}}$. Here, the energy BESS content limits are defined by the installed BESS capacity at the considered node BESS_{cap} and the fixed minimum and maximum per unit limits for the battery state of charge, SoC_{min} and SoC_{max}, respectively. Finally, the charging and discharging power are evaluated according to the energy BESS content $E_{\text{SoC,t}}$ and the BESS efficiency η.

Overall, only local measurements are dictating the real-time operation of all units; the decentralized control scheme is based on Algorithm 1 for the operation of the BESS, the $Q = f(V, P)$ and $P_{\text{curt}} = f(V, P)$ characteristic curves for the inverter-based DER derived from ML, and, following [3], predefined lower and upper voltage limits for the controllable load real-time response. Hence, the evaluation of the real-time operation can be done, by performing power flow calculations considering the local schemes of all units.

IV. CASE STUDY

In order to demonstrate the proposed method, we use the benchmark European radial LV grid described in [23] and depicted in Fig. 3. The installed PV capacity is expressed as a percentage of the total load. PV units are installed on nodes $[12, 16, 18, 19]$ with a corresponding PV share percentage of $[40, 40, 30, 40]$. Furthermore, we consider a 26 kWh BESS and a 5kW CL, whose total daily energy consumption needs to be maintained constant within a day, both installed at Node 16.
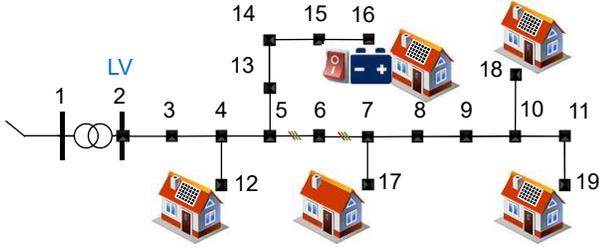
Fig. 3. LV Cigre benchmark grid.
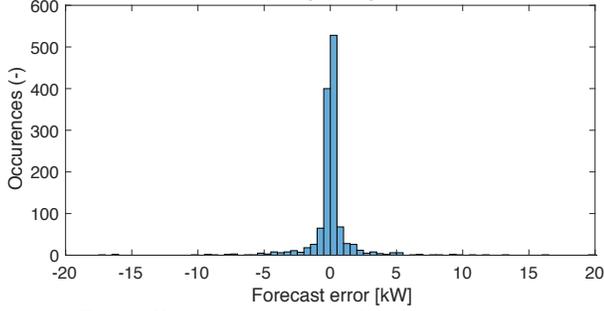
Fig. 4. Histogram of inflexible loads forecast errors.

Fig. 5. Voltage magnitude distribution at all nodes without any control.

TABLE I
FIVE-FOLD CROSS VALIDATION AND FREE PARAMETERS OPTIMIZATION

Node	C	Kernel Type	γ	Polynomial Order
12	4.742	RBF	0.046	−
16	710.250	polynomial	-	4
18	36.243	RBF	0.002	−
19	682.37	polynomial	−	2

All models and parameters regarding costs and constraints are taken from [4]. We assume a maximum acceptable voltage and current magnitude of 1.04 p.u. and 1 p.u., respectively.

Finally, the PV generation uncertainty is taken from [16], which provides the forecast error distribution for 10 PV stations in Switzerland. The forecast error distribution for the loads is computed using a Feed-Forward ANN, as described in Section II. Figure 4 shows the histogram of the hourly load forecast errors for different August days, for all the grid units. The resulting normalized root mean squared error is equal to 1.87%.

Algorithm 1 Proposed BESS rule-based control

Input: $SoC_{min}, SoC_{max}, \eta, P_{load,t}, P_{PV,t}, E_{SoC,t-1}, \text{BESS}_{cap}$
Output: $E_{SoC,t}, P_{gen,t}$
1: **if** $P_{PV,t} \geq P_{l,t}$ **then**
2:     **if** $(P_{PV,t} - P_{l,t}) \cdot \eta \cdot \Delta t \geq (SoC_{max} \cdot \text{BESS}_{cap} - E_{SoC,t-1})$ **then**
3:         $P_{B,t}^{ch} = (SoC_{max} \cdot \text{BESS}_{cap} - E_{SoC,t-1})/\Delta t$
4:         $E_{SoC,t} = E_{SoC,t-1} + P_{B,t}^{ch} \cdot \Delta t$
5:         $P_{net,t} = P_{l,t} + P_{B,t}^{ch}$
6:     **else**
7:         $P_{B,t}^{ch} = (P_{PV,t} - P_{l,t}) \cdot \eta$
8:         $E_{SoC,t} = E_{SoC,t-1} + P_{B,t}^{ch} \cdot \Delta t$
9:         $P_{net,t} = P_{l,t} + P_{B,t}^{ch}$
10:     **end if**
11: **else**
12:     **if** $\frac{P_{l,t} - P_{PV,t}}{\eta} \cdot \Delta t \geq (E_{SoC,t-1} - SoC_{min} \cdot \text{BESS}_{cap})$ **then**
13:         $P_{B,t}^{dis} = (E_{SoC,t-1} - SoC_{min} \cdot \text{BESS}_{cap})/\Delta t$
14:         $E_{SoC,t} = E_{SoC,t-1} - P_{B,t}^{dis} \cdot \Delta t$
15:         $P_{net,t} = P_{l,t} - P_{B,t}^{dis}$
16:     **else**
17:         $P_{B,t}^{dis} = (P_{l,t} - P_{PV,t})/\eta$
18:         $E_{SoC,t} = E_{SoC,t-1} - P_{B,t}^{dis} \cdot \Delta t$
19:         $P_{net,t} = P_{l,t} - P_{B,t}^{dis}$
20:     **end if**
21: **end if**

A. Performance comparison

In this section, we compare the performance of the proposed decentralized control against the centralized BFS-OPF approach and standard local control schemes. Furthermore, we investigate the impact of uncertainty on voltage constraint violations and the behaviour of the available active measures. The following cases are compared:

- *Method 0*: For each time step, an AC PF solution is performed without any control actions. This is the base case.
- *Method 1*: The centralized control scheme based on a multi-period BFS-OPF is used, according to Section II.
- *Method 2*: A decentralized control scheme is used, as described in Section III, without considering uncertainty (i.e., using a deterministic BFS-OPF algorithm to generate the training dataset).
- *Method 3*: A decentralized control scheme is used, as described in Section III, also considering uncertainty (i.e., using a chance-constrained BFS-OPF algorithm to generate the training dataset).
- *Method 4*: The existing local control scheme implemented in Germany according to VDE [11]. The PV generators adjust their power factor according to their active power injections.

First, it can be seen in Fig. 5 that in the absence of any control actions (Method 0), the grid will experience overvoltage. On the contrary, the centralized control (Method 1), based on the multi-period BFS-OPF, corresponds to the optimal behavior of the grid and serves as a benchmark against which the decentralized schemes are compared. However, this method requires extensive monitoring and communication infrastructure.

The characteristic curves of the decentralized control schemes (Methods 2 and 3) are derived based on the SVR approach of Section III. The resulting five-fold cross validation process is given in Table I, along with the corresponding Kernel types and optimized parameters for each PV node. As
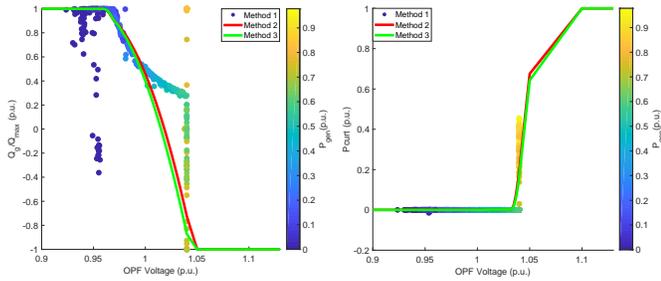
Fig. 6. Characteristic curves $Q = f(V, P)$ and $P_{\text{curt}} = f(V, P)$ at Node 16 according to the SVR procedure in the deterministic (Method 2) and chance-constrained (Method 3) case.
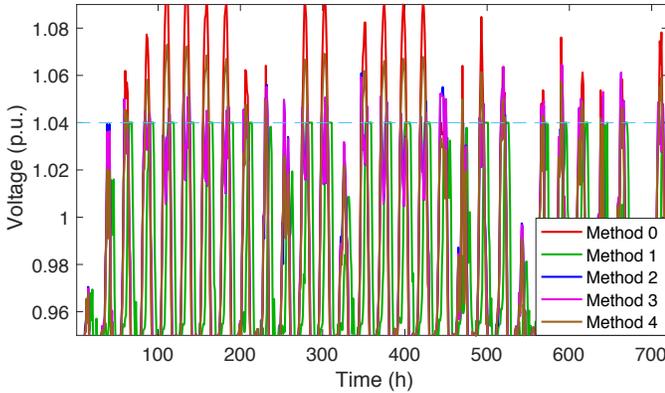
Fig. 7. Voltage evolution at Node 16 with all methods.

described in Section III, some post-processing is necessary to ensure correct behaviour of the units at very low and very high voltages. The characteristic curves for Methods 2 and 3 at Node 16 are shown in Fig. 6 along with the OPF setpoints of the deterministic BFS-OPF. It can been seen that the SVR fitting of Method 3 imposes a slightly more aggressive control for the same voltages compared to Method 2. The larger the acceptable violation probability of the chance-constrained OPF, the larger the difference to the SVR fitting of the deterministic OPF fitting.

Figure 7 shows the evolution of the voltage at the problematic Node 16 over the whole month of June. It can be seen that operating without control (Method 0) or with the current German regulation (Method 4) leads to higher voltage magnitude violations. The OPF-based control scheme (Method 1) satisfies the voltage constraints in an optimal way, relying on extensive monitoring and communication infrastructure. The proposed approaches (Methods 2 and 3) result in some short-term violations, but reduced in magnitude and frequency compared to Method 4.

V. CONCLUSIONS

In this paper, we present a decentralized control scheme for the real-time operation of DERs in active distribution grids. The decentralized scheme is designed using ML techniques on an optimal DER setpoint dataset. The latter is generated with the use of a centralized OPF-based scheme, applied on historical data and considering the generation and load uncertainty. The characteristic curves of the local DER controllers are customized according to the DER location and expected uncertainty based on historical data. In this way, the decentralized control scheme is able to tackle system-wide grid

challenges using purely local controllers, without any remote monitoring and communication infrastructure.

REFERENCES

[1] E. Demirok, P. C. González, K. H. B. Frederiksen, D. Sera, P. Rodriguez, and R. Teodorescu, "Local reactive power control methods for overvoltage prevention of distributed solar inverters in low-voltage grids," *IEEE Journal of Photovoltaics*, vol. 1, no. 2, pp. 174–182, 2011.
[2] R. Tonkoski, L. A. C. Lopes, and T. H. M. El-Fouly, "Coordinated active power curtailment of grid connected PV inverters for overvoltage prevention," *IEEE Transactions on Sustainable Energy*, vol. 2, no. 2, pp. 139–147, 2011.
[3] S. Karagiannopoulos, P. Aristidou, and G. Hug, "Co-optimisation of Planning and Operation for Active Distribution Grids," in *Proceedings of the 12th IEEE Power and Energy Society PowerTech Conference, Manchester*, Jun 2017.
[4] S. Karagiannopoulos, L. Roald, P. Aristidou, and G. Hug, "Operational Planning of Active Distribution Grids under Uncertainty," in *in IREP 2017, X Bulk Power Systems Dynamics and Control Symposium, Espinho*, Aug 2017.
[5] J. Lavaei and S. H. Low, "Zero duality gap in optimal power flow problem," *IEEE Transactions on Power Systems*, vol. 27, no. 1, pp. 92–107, 2012.
[6] S. Bolognani and F. Dörfler, "Fast power system analysis via implicit linearization of the power flow manifold," in *Proc. 53rd Annual Allerton Conference on Communication, Control, and Computing*, 2015.
[7] J. H. Teng, "A direct approach for distribution system load flow solutions," *IEEE Transactions on Power Delivery*, vol. 18, no. 3, pp. 882–887, 2003.
[8] P. Fortenbacher, M. Zellner, and G. Andersson, "Optimal sizing and placement of distributed storage in low voltage networks," in *Proceedings of the 19th Power Systems Computation Conference (PSCC), Genova*, Jun 2016.
[9] S. Karagiannopoulos, P. Aristidou, A. Ulbig, S. Koch, and G. Hug, "Optimal planning of distribution grids considering active power curtailment and reactive power control," *IEEE Power and Energy Society General Meeting*, 2016.
[10] P. Kotsampopoulos, N. Hatziargyriou, B. Bletterie, and G. Lauss, "Review, analysis and recommendations on recent guidelines for the provision of ancillary services by Distributed Generation," in *IEEE International Workshop on Intelligent Energy Systems, IWIES*, 2013, pp. 185–190.
[11] VDE-AR-N 4105, "Power generation systems connected to the LV distribution network." FNN, Tech. Rep., 2011.
[12] S. Weckx, C. Gonzalez, and J. Driesen, "Combined central and local active and reactive power control of PV inverters," *IEEE Transactions on Sustainable Energy*, vol. 5, no. 3, pp. 776–784, 2014.
[13] S. Karagiannopoulos, P. Aristidou, and G. Hug, "Hybrid approach for planning and operating active distribution grids," *IET Generation, Transmission & Distribution*, pp. 685–695, Feb 2017.
[14] O. Sondermeijer, R. Dobbe, D. Arnold, C. Tomlin, and T. Keviczky, "Regression-based inverter control for decentralized optimal power flow and voltage regulation," in *Proceedings of the 2016 IEEE Power and Energy Society General Meeting, Chicago*, 2016.
[15] L. Roald, "Optimization methods to manage uncertainty and risk in power systems operation," Ph.D. dissertation, ETH Zurich, 2016.
[16] Federal office of meteorology and climatology. http://www.meteosuisse.admin.ch/. Accessed: 2016-09-30.
[17] D. O. Mahrufat, A. Ayeni, and A. H. Moshood, "Short term electric load forecasting using neural network and genetic algorithm," *International Journal of Applied Information Systems*, vol. 10, no. 4, pp. 22–28, January 2016, published by Foundation of Computer Science (FCS), NY, USA.
[18] K. Y. Lee, Y. T. Cha, and J. Park, "Short-term load forecasting using an artificial neural network," *Transactions on Power Systems*, vol. 7, no. 1, pp. 124–132, February 1993.
[19] S. Sapna, A. Tamilarasi, M. P. Kumar *et al.*, "Backpropagation learning algorithm based on Levenberg Marquardt Algorithm," *Comp Sci Inform Technol (CS and IT)*, vol. 2, pp. 393–398, 2012.
[20] X. Li, G. Anderson, S. Low, D. Cai, and A. Ulbig, "Comparison of Optimization-based PV Integration Strategies in Southern California," Master's thesis, ETH Zurich, 2015.
[21] J. Snoek, H. Larochelle, and R. P. Adams, "Practical bayesian optimization of machine learning algorithms," in *Advances in neural information processing systems*, 2012, pp. 2951–2959.
[22] K. H. Chua, Y. S. Lim, and S. Morris, "Battery energy storage system for peak shaving and voltage unbalance mitigation," *International Journal of Smart Grid and Clean Energy*, vol. 2, no. 3, pp. 357–363, 2013.
[23] K. Strunz, E. Abbasi, C. Abbey, C. Andrieu, F. Gao, T. Gaunt, A. Gole, N. Hatziargyriou, and R. Iravani, "Benchmark Systems for Network Integration of Renewable and Distributed Energy Resources," *CIGRE, Task Force C6.04*, no. 273, pp. 4–6, 4 2014.